Journal of Marine Science and Technology

Volume 21 | Issue 2 Article 13

ON THE INFLUENCE OF THE MODE-SHAPES OF A MARINE PROPULSION SHAFTING SYSTEM ON THE PREDICTION OF TORSIONAL STRESSES

Bin Tang
Institute of Internal Combustion Engine, Dalian University of Technology, Dalian City, China, btang@dlut.edu.cn

Michael J Brennan
Departamento de Engenharia Mecânica, Universidade Estadual Paulista (UNESP), Ilha Solteira, São Paulo, Brasil.

Recommended Citation

Tang, Bin and Brennan, Michael J (2013) "ON THE INFLUENCE OF THE MODE-SHAPES OF A MARINE PROPULSION SHAFTING SYSTEM ON THE PREDICTION OF TORSIONAL STRESSES," *Journal of Marine Science and Technology*: Vol. 21 : Iss. 2 , Article 13.
DOI: 10.6119/JMST-013-0117-1
Available at: https://jmstt.ntou.edu.tw/journal/vol21/iss2/13

ON THE INFLUENCE OF THE MODE-SHAPES OF A MARINE PROPULSION SHAFTING SYSTEM ON THE PREDICTION OF TORSIONAL STRESSES

Acknowledgements

The first author wishes to acknowledge the financial support from the Doctoral Scientific Research Starting Foundation of Liaoning Province of China (Grant 20091014).

Journal of Marine Science and Technology, Vol. 21, No. 2, pp. 209-214 (2013)
DOI: 10.6119/JMST-013-0117-1

ON THE INFLUENCE OF THE MODE-SHAPES OF A MARINE PROPULSION SHAFTING SYSTEM ON THE PREDICTION OF TORSIONAL STRESSES

Bin Tang[1] and Michael J. Brennan[2]

Key words: torsional vibration, marine shaft, flexible components.

ABSTRACT

Torsional vibration predictions and measurements of a marine propulsion system, which has both damping and a highly flexible coupling, are presented in this paper. Using the conventional approach to stress prediction in the shafting system, the numerical predictions and the experimental torsional vibration stress curves in some parts of the shafting system are found to be quite different. The free torsional vibration characteristics and forced torsional vibration response of the system are analyzed in detail to investigate this phenomenon. It is found that the second to fourth natural modes of the shafting system have significant local deformation. This results in large torsional resonant responses in different sections of the system corresponding to different engine speeds. The results show that when there is significant local deformation in the shafting system for different modes, then multi-point measurements should be made, rather than the conventional method of using a single measurement at the free end of the shaft, to obtain the full torsional vibration characteristics of the shafting system.

I. INTRODUCTION

The torsional vibration of a marine propulsion shafting system may cause shafting failures and should thus be carefully considered at the design stage. The regulations of many shipping registers [2-5] require that torsional vibration of the shafting system should be calculated at the design stage, and then measured during sea trials. There are many instruments available to measure torsional vibration, such as the Geiger torsiograph, the electrical torsiograph, the laser torsiograph and electrical strain-gauging equipment. Electrical torsiographs are widely used nowadays, and the vibration pick-up of this system is usually located at the free-end of the shafting system [11].

Flexible couplings and dampers are often introduced into the marine propulsion shafting system to suppress torsional vibration [20]. The torsional vibration characteristics of such a system are, however, correspondingly more complex. The authors have found that the conventional method of using a single measurement, and then using a model of the shafting system to predict torsional vibration stress can lead to significant errors. Such a situation is illustrated in this paper.

A torsional vibration model of a marine propulsion shafting system with damping and a flexible coupling is first analyzed. The natural frequencies and modes are determined, and the forced torsional vibration response is then calculated using the modal summation method [14]. The forced torsional vibration stress curves obtained from measured vibration at the free end of the propulsion shafting are compared with the results of the forced calculation of the torsional vibration. Significant errors are found for some positions in the shafting system, and so an alternative approach to the prediction method is presented.

II. TORSIONAL VIBRATION CALCULATIONS

Ship shafting systems have traditionally been modeled as a lumped parameter system, a continuous system, or by using three-dimensional finite element models, based on a wealth of practical experience as well as fundamental physical principles. Although there is some recent novel research about the torsional [6, 8, 9, 13, 23], axial [10, 15], transverse [21], and coupled vibration analysis [1, 12, 16, 17], which includes some complex mathematical models, the approximate lumped parameter model is still widely used by engineers. Nestorides [11], Tuplin [19], Wilson [22], and Li *et al*. [7] have reviewed

Paper submitted 01/04/12; revised 09/05/12; accepted 01/17/13. Author for correspondence: Bin Tang (e-mail: btang@dlut.edu.cn).
[1] Institute of Internal Combustion Engine, Dalian University of Technology, Dalian City, China.
[2] Departamento de Engenharia Mecânica, Universidade Estadual Paulista (UNESP), Ilha Solteira, São Paulo, Brasil.

Table 1. Basic parameters of the marine propulsion shafting system.

Parameters	Value
Diesel engine rated power	441 kW
Diesel engine rated speed	1800 rpm
Crankshaft diameter	101.6 mm
Cardan shaft diameter	111.5 mm
Intermediate shaft diameter	89 mm
Propeller shaft diameter	111.5 mm
Speed ratio of engine to propeller	4.041:1

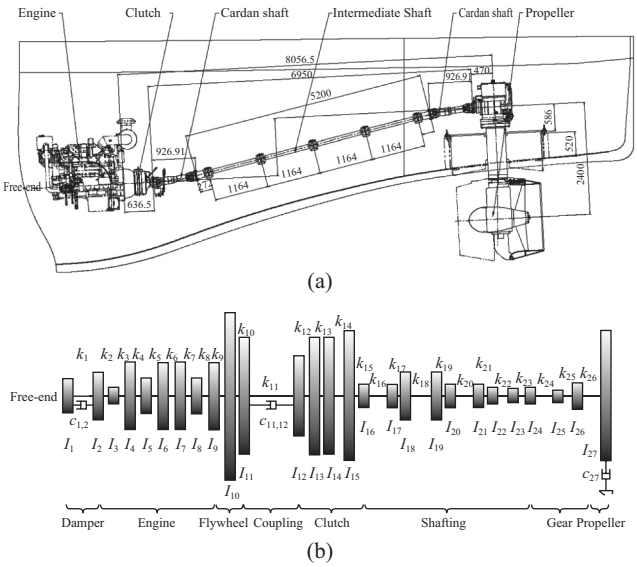

Fig. 1. Marine propulsion shafting system, (a) schematic diagram (in mm), and (b) lumped parameter model.

the methods to establish the equivalent lumped mass models by simplifying the propulsion shafting of marine engine. The schematic diagram of a marine propulsion shafting system driven by a four-stroke, 6 cylinder, diesel engine, and including one damper, one high flexible coupling, and one clutch that is of interest in this paper is shown in Fig. 1(a). The basic parameters of the system are given in Table 1. The approach described in references [7, 11, 19, 22] is used here to construct the lumped parameter model of the propulsion shafting system, in which the lumped inertia elements are connected by massless uniform elastic elements with or without damping elements. Fig. 1(b) shows the simplified lumped mass model with 27 lumped masses; I_i and c_i (i = 1, 2, … 27) are the polar mass moments of inertia and the external damping coefficients of the i-th lumped mass, while $k_{i,i+1}$ and $c_{i,i+1}$ (i = 1, 2, … 27) are the torsional stiffness and the internal damping coefficients of the shaft between inertia elements i and i+1, respectively.

For the lumped mass model, the equation of motion of forced torsional vibrations is given by

Table 2. Natural frequencies of the marine propulsion shafting system.

Modes	Natural frequency (cpm, cycles per minute)
I	488
II	1542
III	5686
IV	8495

$$\mathbf{M}\ddot{\boldsymbol{\theta}} + \mathbf{C}\dot{\boldsymbol{\theta}} + \mathbf{K}\boldsymbol{\theta} = \mathbf{t} \tag{1}$$

where **M** is the diagonal inertia matrix, and **C** and **K** are the symmetric damping and stiffness matrices respectively. If the marine propulsion shafting has a simple configuration without any branches, the damping and stiffness matrixes are tri-diagonal. For multi-branched systems, the damping and stiffness elements can be defined according to the methods given in [18]. The angular displacement and excitation torque vectors are given by **θ** and **t** respectively. Detailed information on the Fourier analysis of the crankpin tangential force and the method to establish the equation of motion can be found in [7, 11, 19, 22].

To obtain the equation of motion for the undamped free torsional vibration of the system, the damping and the excitation torque are set to zero, i.e., **C** = 0 and **t** = 0. The resulting system of equations corresponds to an eigenvalue problem, which can be solved easily to give the natural frequencies and mode-shapes of the system. The first four natural frequencies are tabulated in Table 2, and the corresponding mode-shapes are shown in Fig. 2. Note that they are plotted using a logarithmic scale as the relative amplitudes between various positions can be very large. Note also, that as the modulus of the mode-shapes is plotted, the positive and negative angular displacements are indicated by different line-styles.

The relative elastic torque between the inertia elements at each frequency $T_{i,i+1} = (\Theta_{i+1} - \Theta_i)k_{i,i+1}$, where Θ_i is the amplitude of the relative free torsional vibration at each inertia mass for a unit degree rotation amplitude at the free-end of the shafting system.

The relationship between the various orders of engine speed and excitation frequency is shown in Fig. 3. The straight lines represent each half order and the first four natural frequencies are shown by horizontal lines. The speeds corresponding to resonance frequencies occur at the intersection of the horizontal lines and the engine-order lines.

The forced torsional vibration response can be obtained using the modal summation method [14] to give

$$\frac{\Theta_{r,s}}{T_s} = \sum_{n=1}^{N} \frac{\psi_{n,r}\psi_{n,s}}{m_n\left(\omega_n^2 - \omega^2 + j2\zeta_n\omega\omega_n\right)} \tag{2}$$

where $\Theta_{r,s}$ is the amplitude at the r-th position due to the

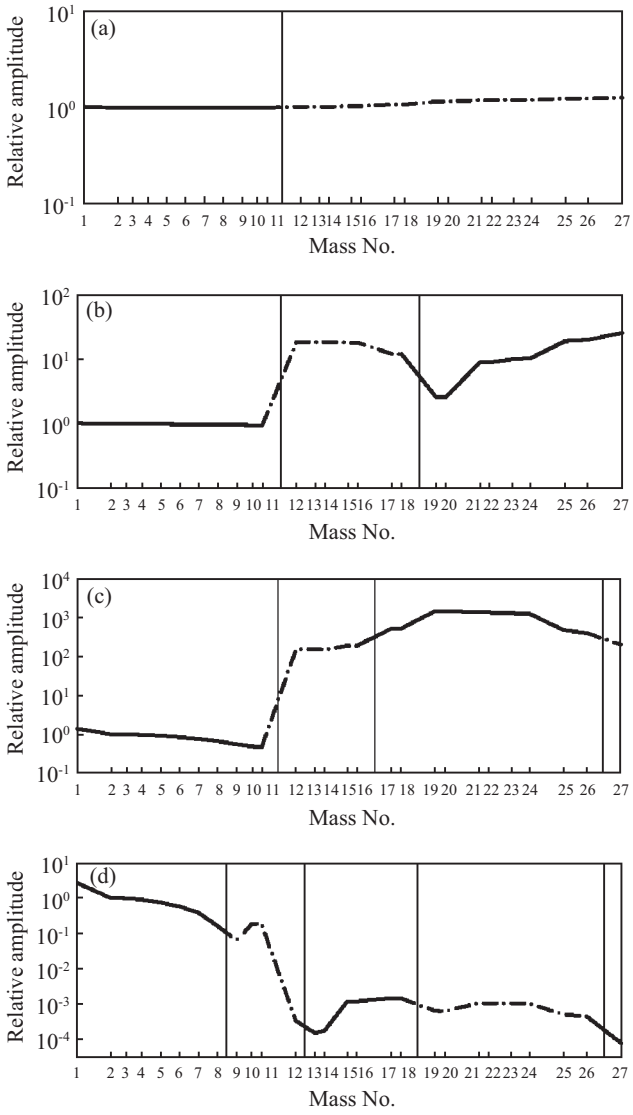

Fig. 2. Mode shapes of the marine propulsion shafting: (a) first mode, (b) second mode, (c) third mode, and (d) fourth mode. When the relative amplitude changes from solid line to dash-dotted line, the phase of mode-shapes changes. Thin solid vertical lines indicate the positions at which the phase of the mode-shapes changes.

torque amplitude T_s at the *s*-th position; ω is the excitation frequency; $\psi_{n,r}$ is the *n*-th mode shape evaluated at the *r*-th position; ω_n, m_n, and ζ_n are *n*-th the circular natural frequency, modal mass and damping ratio respectively.

The predicted torque $M_i = k_{i,i+1}(\theta_{i+1} - \theta_i)$, which is within the *i*-th massless uniform elastic shaft element between the two lumped inertia masses *i* and *i*+1, can be obtained from the forced response at different engine working conditions. The predicted torsional vibration stress within each massless uniform elastic shaft element $\tau_i = M_i / W_{i,i+1}$, where $W_{i,i+1}$ is the sectional modulus of the *i*-th length of shaft. The torsional vibration stress curves for the crankshaft and propeller shaft are shown in Fig. 4. The primary orders of vibration, such as

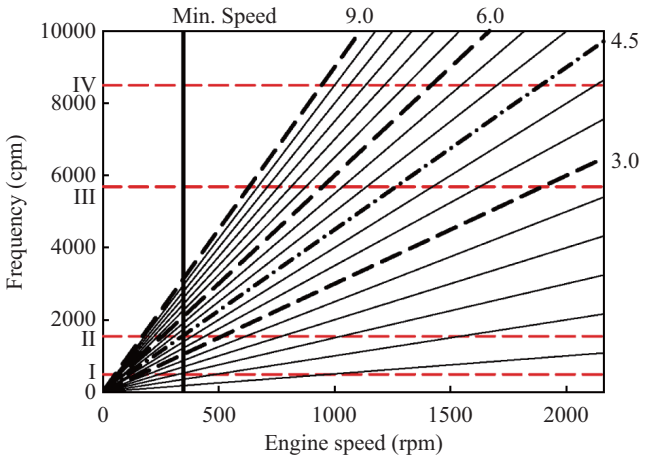

Fig. 3. Campbell diagram for the prolusion system, I: first mode; II: second mode; III: third mode; IV: fourth mode. 3.0, 4.5, 6.0, and 9.0 are the primary shaft orders.

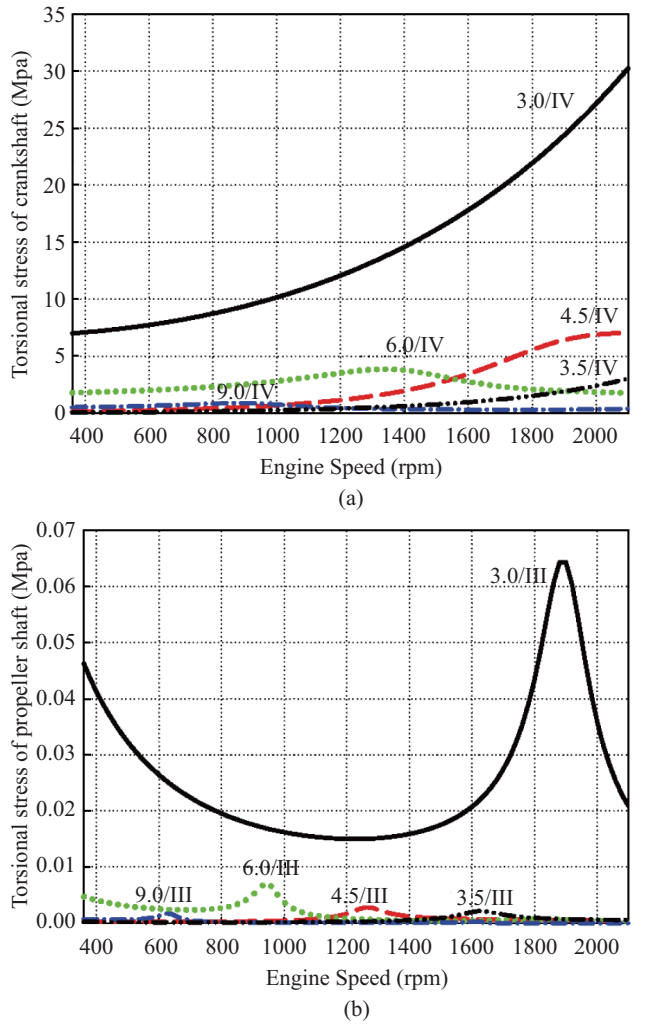

Fig. 4. Torsional stress curves for the (a) crankshaft and (b) propeller shaft. Solid line —, 3.0 order; dashed-dotted-dotted line −···−, 3.5 order; dashed line − −, 4.5 order; dotted line ·····, 6.0 order; dashed-dotted line −·−, 9.0 order. III, third mode; IV, fourth mode.

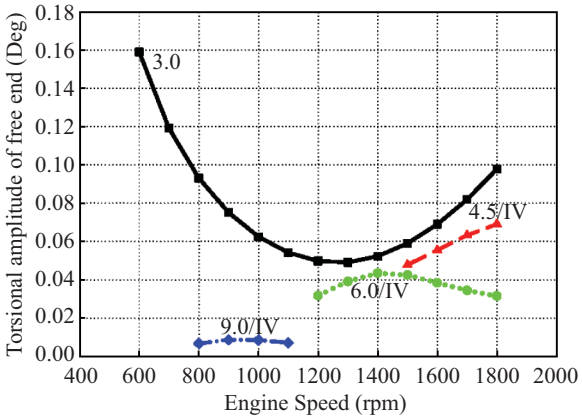

Fig. 5. Measured torsional amplitude at the free end of the marine propulsion shafting. Solid line −■−, 3.0 order; dashed line −▲−−, 4.5 order; dotted line ··●··, 6.0 order; dashed-dotted line −♦·−, 9.0 order. IV, fourth mode.

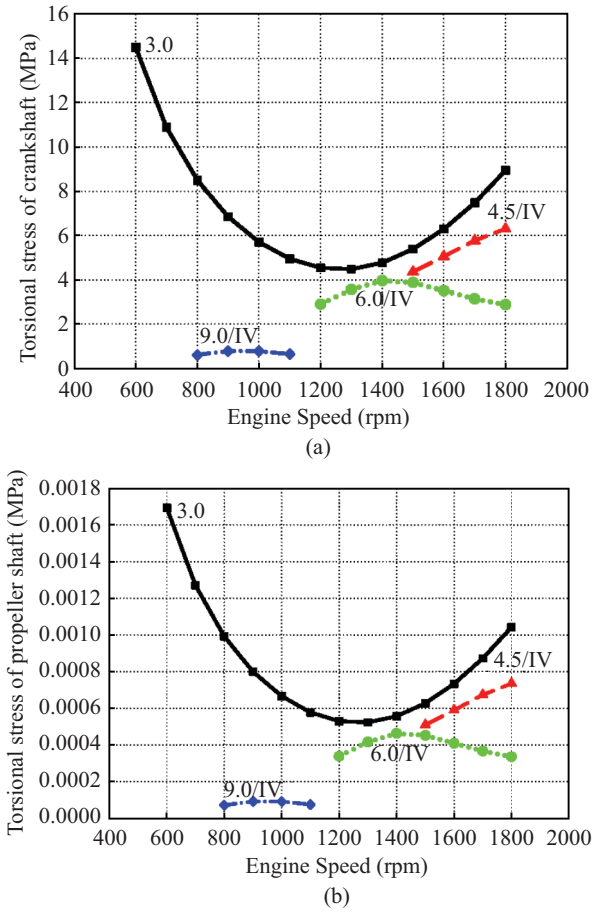

Fig. 6. Predicted torsional stresses using the measured data at the free end and the lumped parameter model for the (a) crankshaft and (b) propeller shaft. Solid line −■−, 3.0 order; dashed line −▲−−, 4.5 order; dotted line ··●··, 6.0 order; dashed-dotted line −♦·−, 9.0 order. IV, fourth mode.

3.0, 4.5, 6.0, 9.0 orders etc., are given between 360 and 2100 rpm. The notation in Fig. 4 and subsequent figures, for example 3.0/IV, indicates the peak response corresponding to the IV mode due to the third primary shaft order. It can be seen that in the crankshaft 3.0, 4.5, 6.0 and 9.0 orders fourth-mode (IV) are dominant orders. It can also be noticed that in the propeller shaft the 3.0, 4.5, 6.0 and 9.0 orders third-mode (III) are dominant orders. The rigid-body motion of the crankshaft, in which there is negligible relative angular motion between the inertia elements at the low speed range, is related to the 3.0 shaft order. In the literature this is also called rolling vibration [7, 22].

III. MEASUREMENT OF THE TORSIONAL VIBRATION AND DISCUSSION

When the torsiograph sensor is located at the free-end of the shafting, the torsional vibration of the propulsion shafting over the whole operating speed range can be predicted using the model. The measurement was carried out during normal steady-state operating conditions. The engine was run between 600 rpm and 1800 rpm, with a speed interval of 50 rpm when the system was not resonant and 20 rpm for speeds close to the resonance frequencies. The vibration at the free-end of the system was measured using an ANZT torsional vibration meter with maximum sampling frequency of 600 kHz at each engine speed. Fourier analysis of the data was carried out to determine the orders and the Campbell diagram in Fig. 3 was used to determine the dominant modes of vibration. The measured forced vibration amplitudes at the free-end of the propulsion shafting are shown in Fig. 5. It can be seen that the 3.0, 4.5, 6.0 and 9.0 orders fourth-mode are dominant orders, and the 6.0 order fourth mode peak at about 1400 rpm indicates the fourth mode resonant frequency is approximately 8400 cpm.

The measured torsional vibration stress curves are obtained by using the measured torsional vibration amplitude A_i at the free end of the propulsion shafting and the relative elastic torque $T_{i,i+1}$. The experimental torsional vibration stress at the i-i+1 shaft $\tau_{i,i+1} = T_{i,i+1} A_i / W_{i,i+1}$. The predicted torsional vibration stresses in the crankshaft and propeller using the measured data and the model of the shafting system are shown in Fig. 6. Comparing these curves with the calculated curves given in Fig. 4, it can be seen that the 3.0, 4.5, 6.0 and 9.0 orders fourth-mode stress curves in both the crankshaft and the propeller shaft calculated from the measured data are dominant. The rigid-body motion of the crankshaft at the low speed range is also notable. Except for the rigid-body motion, the stress curves in the crankshaft are reasonably coincident with those in Fig. 4(a), but this is not the case for the propeller shaft, which can be seen by comparing Figs. 4(b) and 6(b).

The reason for this may be seen by studying the relative amplitudes of the mode-shapes given in Fig. 2. It can be seen that the relative free torsional vibration amplitudes at the free-end and the propeller end are very different in the second

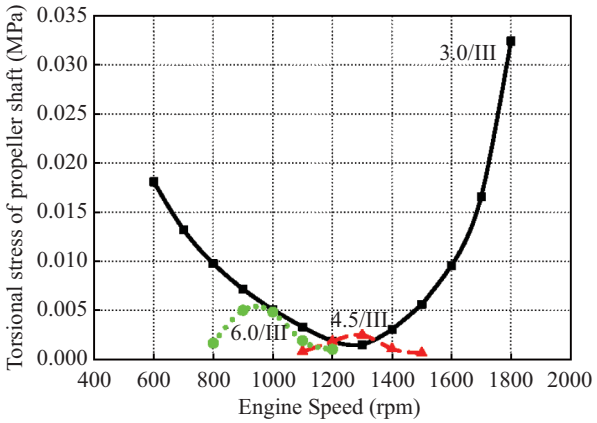

Fig. 7. Torsional stress curves according to the "measured" stress on the no. 16-17 for the propeller shaft. Solid line −■−, 3.0 order; dashed line −▲−−, 4.5 order; dotted line ··●··, 6.0 order; dashed-dotted line −♦·−, 9.0 order. III, third mode.

to fourth modes, the maximum difference being a factor of 1000.

It is clear that in the second to the fourth modes the motion of the crankshaft is largely decoupled from the propeller shaft. It is also clear that in the fourth mode the motion is much larger at the free end than at the propeller end, which contrasts with the second and third modes. Thus if a measurement is made at the free-end, it will be dominated by the fourth mode, with the second and third modes being difficult to detect. As seen in Fig. 4(b), however, the dominant stress at the propeller end is due to the third mode, and this will be difficult to predict from a single measurement at the free-end, as vibration of the third mode will be negligibly small in any measurement at the free-end.

To obtain the torsional vibration stress or torque curves of shaft, the torsional strain at some position on the shaft should be measured. To illustrate this some simulations were carried out using the model. Torsional stress at shaft no. 16-17 was obtained from the model, as if it had been obtained experimentally and the torsional stress curves for the marine propulsion system calculated with reference to this data. The predicted stress at the propeller end is shown in Fig. 7. It can be seen that it compares well with the predictions in Fig. 4(b). It can be noticed that the 3.0, 4.5 and 6.0 order third-mode stress curves are now dominant. The 6.0 order third mode peak at about 950 rpm indicates that the third mode resonant frequency is approximately 5700 cpm.

IV. CONCLUSIONS

The torsional vibration of a marine propulsion system with several highly flexible components has been investigated in this paper. The results show that a highly flexible component may have a significant effect on the mode-shapes, effectively dynamically decoupling one end of the system from the other. If there are local mode resonant engine speeds over the whole marine propulsion operating range, the traditional measurement method, which is measuring vibration at the free end of the shafting system, may lead to large errors in the prediction of maximum stresses in the shaft. If this is the case, then to avoid such errors measurements are needed at both the free end and on the shaft.

ACKNOWLEDGMENTS

The first author wishes to acknowledge the financial support from the Doctoral Scientific Research Starting Foundation of Liaoning Province of China (Grant 20091014).

REFERENCES

1. Boysal, A. and Rahnejat, H., "Torsional vibration analysis of a multi-body single cylinder internal combustion engine model," *Applied Mathematical Modelling*, Vol. 21, No. 8, pp. 481-493 (1997).
2. Bureau Veritas, *BV Rules for the Classification of Steel Ships*, Part C Machinery, Electricity, Automation and Fire Protection, Chapter 1 Machinery, Section 9 Shaft Vibrations, Article 3 Torsional Vibrations (2011).
3. China Classification Society, *CCS Rules for Classification of Sea-going Steel Ships*, Part 3 Machinery Installations, Chapter 12 Shaft Vibration and Alignment, Section 2 Torsional Vibration (2009).
4. Det Norske Veritas, *DNV Rules for Classification of Ships*, Part 4 Machinery and systems – main class, Chapter 3 Rotating Machinery, Drivers, Section 1 Diesel Engines, G. Vibration (2009).
5. Germanischer Lloyd, *GL Rules for Classification and Construction Ship Technology*, Part 1 Seagoing Ships, Chapter 2 Machinery Installations, Section 16 Torsional Vibrations (2009).
6. Guzzomi, A. L., Hesterman, D. C., and Stone, B. J., "Some effects of piston friction and crank or gudgeon pin offset on crankshaft torsional vibration," *Journal of Ship Research*, Vol. 54, No. 1, pp. 41-52 (2010).
7. Li, B. Z., Chen, Z. Y., and Ying, Q. G., *The Torsional Vibration of Internal Combustion Engine Shafting*, National Defence Industry Press, Beijing (1984).
8. Magazinović, G., "Regression-based assessment of shafting torsional vibration key responses," *Marine Technology*, Vol. 47, No. 1, pp. 65-73 (2010).
9. Mendes, A. S., Meirelles, P. S., and Zampieri, D. E., "Analysis of torsional vibration in internal combustion engines: modelling and experimental validation," *Proceedings of the Institution of Mechanical Engineers, Part K: Journal of Multi-body Dynamics*, Vol. 222, No. 2, pp. 155-178 (2008).
10. Murawshi, L., "Axial vibrations of a propulsion system taking into account the couplings and the boundary conditions," *Journal of Marine Science and Technology*, Vol. 9, No. 4, pp. 171-181 (2004).
11. Nestorides, E. J., *A Handbook on Torsional Vibration*, Cambridge University Press, Cambridge (1958).
12. Offner, G., Eizenberger, T., and Priebsch, H. H., "Separation of reference motions and elastic deformations in an elastic multi-body system," *Proceedings of the Institution of Mechanical Engineers, Part K: Journal of Multi-body Dynamics*, Vol. 220, No. 1, pp. 63-75 (2006).
13. Pasricha, M. S., "Effect of damping on parametrically excited torsional vibrations of reciprocating engines including gas forces," *Journal of Ship Research*, Vol. 50, No. 2, pp. 147-157 (2006).
14. Rao, S. S., *Mechanical Vibrations, 4th Ed.*, Pearson Education, New Jersey (2004).
15. Shu, G. Q., Liang, X. Y., and Lu, X. C., "Axial vibration of high-speed automotive engine crankshaft," *International Journal of Vehicle Design*, Vol. 45, No. 4, pp. 542-554 (2007).
16. Tang, B., "Dynamic analysis of crankshafts using dynamic stiffness matrix," *Journal of Ship Mechanics* (*English Edition*), Vol. 13, No. 3, pp. 465-476 (2009).

17. Tang, B. “Continuum element method for analysing free-vibration behaviour of crankshafts,” *Proceedings of the Institution of Mechanical Engineers, Part D: Journal of Automobile Engineering*, Vol. 223, No. 1, pp. 49-64 (2009).
18. Tang, B., Xue, D. X., and Song, X. G., “Review of torsional vibration analysis of multi-branched shaft systems,” *Noise and Vibration Control*, Vol. 29, No. 3, pp. 1-5 (2009).
19. Tuplin, W. A., *Torsional Vibration*, Chapman & Hall, London (1934).
20. Wang, L. X., “The action of the high flexible rubber coupling on the property of torsional vibration,” *Journal of Dalian University of Technology*, Vol. 18, No. 4, pp. 69-85 (1978).
21. Warikoo, R. and Haddara, M. R., “Analysis of propeller shaft transverse vibrations,” *Marine Structures*, Vol. 5, No. 4, pp. 255-279 (1992).
22. Wilson, W. K., *Practical Solution of Torsional Vibration Problems* (*Five Volumes*), Chapman & Hall, London (1963).
23. Zhang, X. and Yu, S. D., “Torsional vibration of crankshaft in an engine-propeller nonlinear dynamical system,” *Journal of Sound and Vibration*, Vol. 319, Nos. 1-2, pp. 491-514 (2009).